

# Electrochemical sensor based on molecularly imprinted polymer and graphene oxide nanocomposite for monitoring glyphosate content in corn

Xuejiao Ren, Hui Zeng, Qiyuan Zhang, Hongyu Cai, Wei Yang\*

Faculty of agronomy, Jilin Agricultural University, Changchun, 130118, China

\*E-mails: [davidyoung588@sina.com](mailto:davidyoung588@sina.com)

Received: 1 November 2022 / Accepted: 2 December 2022 / Published: 27 December 2022

The current study has been focused on the preparation of an electrochemical sensor based on molecularly imprinted polymer and graphene oxide nanocomposite modified glassy carbon electrode (MIP@GO/GCE) for monitoring glyphosate (GPh) content in corn. The MIP-based nanocomposite was prepared through the polymerization of pyrrole on GO nanosheets. The structural studies of synthesized MIP-based nanocomposite by SEM and XRD analyses indicated effective polymerization PPy on the surface of GO. Electrochemical analyses demonstrated that MIP@GO/GCE showed the sensitive and selective electrocatalytic response to GPh in electrochemical cells, and indicated a sensitivity of 0.1271  $\mu\text{A}/\mu\text{M}$  and a stable linear range from 0 to 1800  $\mu\text{M}$ . The sensor for GPh reached a low detection limit of 11  $\mu\text{M}$ . The results revealed that MIP@GO/GCE possessed the broad linear range and relatively low detection limit value between the recent GPh sensors. The applicability and validity of the MIP@GO/GCE as GPh sensor in food samples was examined and results exhibited that the obtained recovery (97.00% to 98.25%) and RSD (3.58% to 4.25%) values were acceptable. It reflected the appropriate accuracy and validity of results of MIP@GO/GCE for the determination of GPh level in food samples.

**Keywords:** Glyphosate; Molecularly Imprinted Polymer; Food Samples; Nanocomposite; Graphene Oxide; Electrochemical Techniques

## 1. INTRODUCTION

Glyphosate (GPh; 2-(phosphonomethylamino)acetic acid) commonly known as Roundup is a broad-spectrum systemic and non-selective herbicide, meaning it will kill most plants such as weeds, especially annual broadleaf weeds and grasses that compete with crops. It prevents the plants from making specific proteins are needed for plant growth. GPh is an organophosphorus compound that acts by inhibiting the plant enzyme 5-enolpyruvylshikimate-3-phosphate synthase [1, 2]. GPh can cause

imbalances in gut bacteria and some reports have indicated that GPh appears to accumulate in human cells and is suspected of causing genetic damage [3, 4]. At low concentrations, it damages the liver, kidney and skin cells and long-term effects include cancer, infertility, pregnancy problems, birth defects and respiratory diseases [5-7]. GPh is acutely toxic to fish and birds and can kill beneficial insects such as bees and soil organisms that maintain ecological balance [8-10]. Laboratory studies have identified adverse effects of GPh-containing products in all standard categories of toxicological testing [11]. Biologists have sounded the alarm over the serious decline in insect populations that affect species diversity [8, 12, 13].

As a result, the determination of GPh level in food and water specimens is a very important issue. Ion chromatography [14], enzyme-linked immunosorbent assay [15], mass spectrometry [16], fluorescent probes [17], high-performance liquid chromatography [18], capillary gas chromatography [19], spectrophotometry [20] and electrochemical sensors [21-25] are the traditional techniques for determination GPh concentration. However, most of these methods are is economical challenging and time-consuming [26-28]. Among these techniques, electrochemical techniques proved to be more economic and sensitive, and provided appropriate precision and selectivity for GPh determination in food and water samples. However, further researches require to advance the sensing performance of GPh electrochemical sensors. Thus, the current study has been focused on preparation electrochemical sensor based on molecularly imprinted polymer and graphene oxide nanocomposite for monitoring GPh content in corn.

## 2. EXPERIMENT

### 2.1. Preparation of molecularly imprinted polymeric electrode

For preparation of the MIP@GO/GCE [29], 1.5 mM pyrrole (98%, Sigma-Aldrich) and 5 mL isopropanol ( $\geq 99.8\%$ , Merck, Germany) solution containing 0.5 mM GPh (Sigma-Aldrich) were ultrasonically mixed for 60 minutes at 25°C. After pre-assembly of template molecules and monomers, 0.20 GO were ultrasonically dispersed in a mixture of 30 mL 2.5 M hydrochloride acid (37%, Sigma-Aldrich) and 10 mL of isopropanol. After 25 minutes sonication, 0.7 mM  $\text{FeCl}_3 \cdot 6\text{H}_2\text{O}$  (99%, Merck, Germany) was added to the mixture into the GO dispersion for polymerization the pyrrole under magnetic stirring for 4 hours to obtain the homogenous black mixture. Next, the obtained mixture was centrifuged at 1000 rpm for 10 minutes to collect the resultant precipitates which were rinsed with deionized water several times and dried in an oven at 70 °C for 10 hours. The dried depositions as MIP@GO were stored in a 4 °C refrigerator. Prior to the modification of the GCE, bare GCE (3mm in diameter) was thoroughly polished with 0.3  $\mu\text{m}$   $\text{Al}_2\text{O}_3$  slurry (99%, Zhengzhou Haixu Abrasives Co., Ltd. China) on micro-cloth pads to obtain a mirror-like surface, then rinsed thoroughly with ethanol and deionized water for several times. 10 mL of 10g/L MIP@GO suspension was carefully cast on the clean surface of GCE and dried at room temperature. Afterward, chronoamperometry at a potential of 1.2 V for 10 minutes in 0.1 M phosphate buffer solution (PBS) with pH 5.0 using electrochemical workstation (Zhengzhou CY Scientific Instrument Co., Ltd., China) was employed for remove the template molecules. The electrochemical workstation was equipped conventional three-electrode system

containing the modified GCE, platinum plate and Ag/AgCl (3 M KCl) as the working, counter, and reference electrode, respectively. Thereby, the MIP@GO/GCE with substantial number of molecular binding sites was achieved. For control, the nonimprinted PPy@GO/GCE (NIP@GO/GCE) was prepared in the same method without additional template (GPh), and MIP/GCE and GO/GCE samples were prepared without the addition of GO and MIP, respectively.

## 2.2. Characterization instruments

An electrochemical workstation (Xian Yima Optoelec Co., Ltd., China) was used for electrochemical analyses based on differential pulse voltammetry (DPV) techniques in 0.1 M PBS with pH 7.0 as the supporting electrolyte. The electrolyte was prepared using a stock solution of 0.1 M  $\text{KH}_2\text{PO}_4$  ( $\geq 98.0\%$ , Sigma Aldrich). Scanning electron microscopy (SEM, JEOL JXA8600 M) and X-ray diffractometer (XRD, Philips X-pert Pro PW 1830 with CuK $\alpha$  radiation) were employed for characterization the crystallographic and morphological information of the synthesized nanomaterial, respectively.

## 2.3. Preparation of the actual sample from Corn samples

Corn samples were purchased from the local markets in Changchun, Jilin Province, China. 10 g of pesticide free ground corn was mixed with 150 mL of 0.1 M PBS (pH 7.0). After sonication for 30 minutes at room temperature, the mixture was put in the refrigerator for 48 hours. Subsequently, the mixture ultrasonically blended for 30 minutes at room temperature. Next, the mixture was filtered, and then centrifuged at 2000 rpm for 20 min to collect the residues. After then, the liquid extracts was used for electrochemical studies. Glyphosate ELISA Plate Kit (Eurofins Abraxis, USA) was used for determination GPh in prepared real samples.

# 3. RESULTS AND DISCUSSION

## 3.1. Structural studies of synthesized molecularly imprinted polymeric electrode

The XRD spectra of powders of MIP, GO, MIP@GO and NIP@GO are exhibited in Figure 1. As seen from XRD spectra of MIP, there are the conventional scattering of the X-ray beams that forms a very broad peak from  $2\theta = 5$  to  $20^\circ$ , indicating characteristics of MIP amorphous nature [30, 31]. XRD spectra of GO show the typical (001) and (100) diffraction peaks of GO that are obtained at  $2\theta = 10.19^\circ$  and  $41.77^\circ$ , respectively [32-34]. XRD spectra of the MIP@GO and NIP@GO show the (100) peak of GO is disappeared and (001) peak of GO becomes weaker and broader which can be attributed to the superimposition of peaks of the GO with a large band of the PPy [35-37], indicating to successful polymerization of PPy on the surface of GO [38].

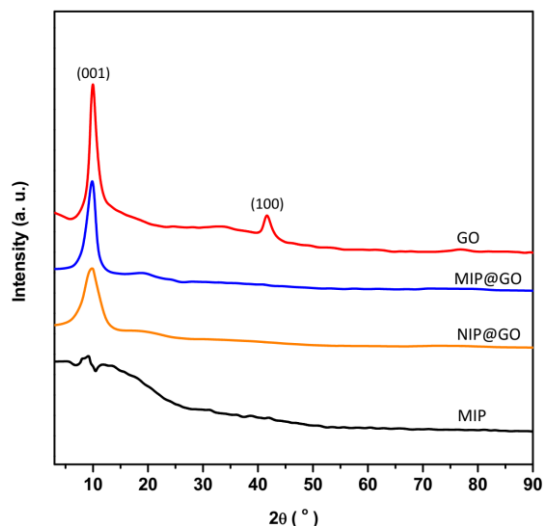


**Figure 1.** The XRD spectra of powders of MIP, GO, MIP@GO and NIP@GO.

SEM micrographs of the GO/GCE, MIP@GO/GCE and NIP@GO/GCE are displayed in Figure 2. SEM micrograph of the GO/GCE in Figure 2a exhibits the curved, layer morphology with smooth surfaces of GO nanosheets. SEM micrograph of NIP@GO/GCE shows GO nanosheets with NIP with rough surfaces on nanosheets. In contrast, the SEM micrograph of MIP@GO/GCE shows that the morphological structures of the modified electrode have higher porosity, roughness and bulging which indicates an effective polymerization of MIP film on the nanosheets of GO [39-41].

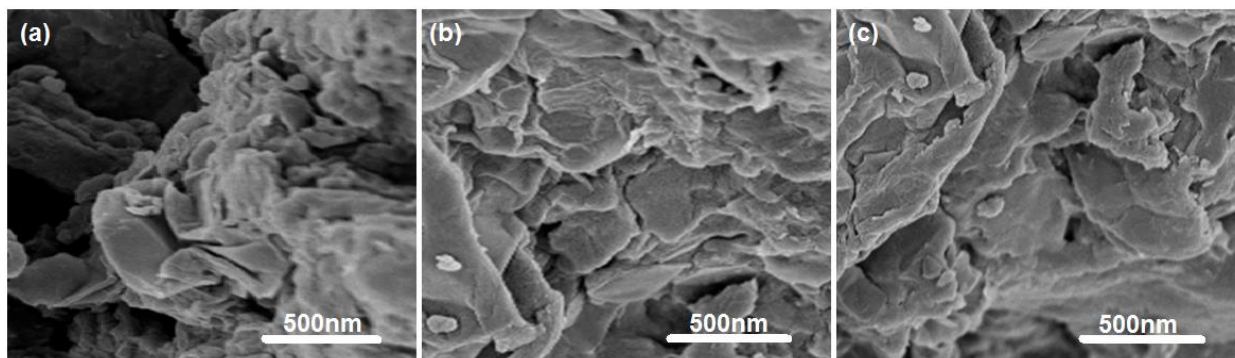


**Figure 2.** SEM micrographs of the (a) GO/GCE, (b) MIP@GO/GCE and (c) NIP@GO/GCE.

### 3.2. Electrochemical studies

DPV curves MIP/GCE, GO/GCE, MIP@GO/GCE, NIP@GO/GCE and GCE at applied potentials between 0.40 V to 1.15 V in  $25 \text{ mVs}^{-1}$  scan rate into 0.1M PBS (pH=7.0) containing  $350 \mu\text{M}$  GPh are depicted in Figure 3. As seen, the DPV curves MIP/GCE, GO/GCE, MIP@GO/GCE and NIP@GO/GCE show an anodic oxidation peak at 0.96 V, 0.99 V, 0.94 V and 0.98 V, respectively, that the peak can be related to the irreversible oxidation of the secondary amine [42-44]. The DPV curves of GCE do not show any obvious peak. It is observed that MIP@GO/GCE shows a significant

electrocatalytic peak current and lower oxidation potential than that other electrodes. It illustrates that nanocomposite of molecularly imprinted polymer on nanosheets of GO which act as the supporting nanostructure for MIP to form binding sites at the nanosheet surface as well as great effective surface, good stability and easy functionalization improve the affinity and sensitivity of sensor. The GO nanosheets can promote the conductivity and density of imprinted sites located in the curved and layer of GO [45-47]. It can be considered a guarantee for great effective specific recognition and leads to the enhancement of signal response of MIP@GO/GCE [48]. Furthermore, the porous, rough and bulging morphology of MIP@GO/GCE facilitates the diffusion rate and improve the electrochemical reactions rate [49-51]. The carboxyl and phosphate groups of GPh as an anionic state show a great affinity to the PPy sites [52-54]. Additionally, MIP exhibits characteristics complementary to the spatial structure of the GPh molecule that the imprinted cavities provide binding sites with high affinity and selectivity to recognize the target molecules [55-57]. MIP based sensor indicates a higher electrochemical signal of GPh than that NIP based sensor, reflecting the great specific adsorption of MIP towards GPh molecule because of the presence of higher porosity and roughness and higher density of imprinted cavities in the MIP than that NIP [58, 59]. The results are consistent with the SEM analyses of MIP@GO/GCE and NIP@GO/GCE. Thus, the following electrochemical analyses were conducted on MIP@GO/GCE.

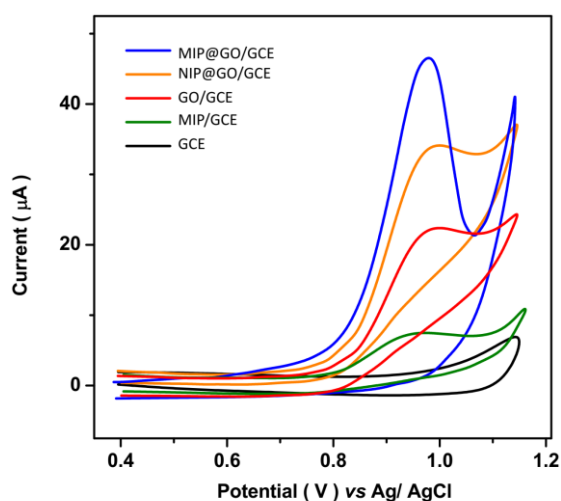


**Figure 3.** DPV curves MIP/GCE, GO/GCE, MIP@GO/GCE, NIP@GO/GCE and GCE at applied potentials between 0.40 V to 1.15 V in scan rate of  $25 \text{ mVs}^{-1}$  in 0.1 M PBS (pH 7.0) containing  $350 \mu\text{M}$  GPh.

Figure 4a depicts the DPV response of MIP@GO/GCE under consecutive injections of  $200 \mu\text{M}$  GPh solutions in an electrochemical cell containing 0.1 M PBS (pH 7.0), at applied potentials from 0.40 V to 1.15 V in a scan rate of  $25 \text{ mVs}^{-1}$ . The DPV response of MIP@GO/GCE demonstrates that after each injections of  $200 \mu\text{M}$  GPh solution, the DPV peak current is increased, reflecting excellent response of MIP@GO/GCE toward GPh. Figure 4b shows the corresponding calibration plot that indicates the sensitivity of  $0.1271 \mu\text{A}/\mu\text{M}$  and a stable linear range from 0 to  $1800 \mu\text{M}$ . The sensor for GPh reaches a low detection limit of 11 nM. The electrochemical sensor performance for determination GPh in current

study and other reports in the literature are summarized in Table 1, illustrating that MIP@GO/GCE possesses a broad linear range and relatively low detection limit value between the recent GPh sensors. It can be related to a synergism exists between the GO and MIP [60-62], that can provide electro-conducting path and excellent surface-to-volume to promote the accessibility of the GPh molecule to the binding sites and cavities and facilitates the electron transfer rate [63-65].

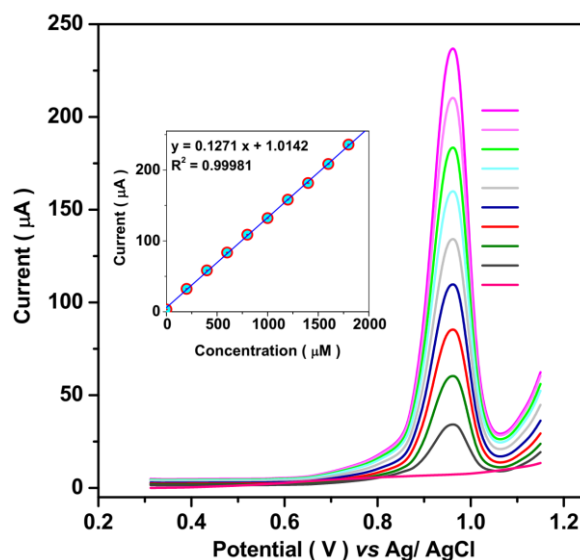


**Figure 4.** DPV response and the equivalent calibration plots of MIP@GO/GCE under consecutive injections of 200  $\mu\text{M}$  GPh solutions in an electrochemical cell containing 0.1 M PBS (pH 7.0), at applied potentials from 0.40 V to 1.15 V in a scan rate of 25  $\text{mVs}^{-1}$ .

**Table 1.** The electrochemical sensor performance for determination GPh in current study and other reports in the literature.

Electrodes	Method	Linear range ( $\mu\text{M}$ )	Detection limit ( $\mu\text{M}$ )	Ref.
MIP@GO/GCE	DPV	0–1800	11	This work
CuCl doped graphene/double-walled carbon nanotubes	DPV	$6 \times 10^{-6}$ –0.3	$0.77 \times 10^{-5}$	[21]
CuO/ionic liquid/hollow fiber/MWCNTs/pencil graphite electrode	DPV	0.005–1.1	1.3	[22]
Graphite oxide paste electrode	SWV	18–1200	17	[42]
CuAl graphene nanoprobe	DPV	0.0029–1.18	1	[23]
Nanoporous copper	CV	0.030–0.065	4	[66]
rGO/double-Walled CNTs/octahedral- $\text{Fe}_3\text{O}_4$ /chitosan / screen-printed gold electrodes	SWV	$6 \times 10^{-4}$ –6	0.47	[67]
Copper benzene-1,3,5-tricarboxylate nanocomposite	DPV	$10^{-7}$ –1	$2.6 \times 10^{-5}$	[68]

SWV: Square Wave Voltammetry

For evaluation of the specificity of proposed GPh sensing method, the DPV response of MIP@GO/GCE under consecutive injections of 10  $\mu\text{M}$  GPh solution and 40  $\mu\text{M}$  interfering compounds presence in food samples in an electrochemical cell containing 0.1 M PBS (pH 7.0), at applied potentials from 0.40 V to 1.15 V in a scan rate of 25  $\text{mVs}^{-1}$  were investigated. The results of electrocatalytic peak current of DPV measurements at 0.94 V are listed in Table 2. These findings show that there is a substantial electrocatalytic response of MIP@GO/GCE to the addition of GPh in electrochemical cell. Meanwhile, it is not observed any significant electrocatalytic response under addition interfering substances into the electrolyte solution. It reveals that MIP-based GPh in this study can specifically recognize the target molecules due to the specific cavities designed for a target molecule in the MIP matrix which provides strong interaction between the target molecule and binding sites to determine the selectivity of MIP [69, 70].

**Table 2.** Results of electrocatalytic peak current of DPV measurements at 0.94 V using MIP@GO/GCE under consecutive injections of 10  $\mu\text{M}$  GPh solution and 40  $\mu\text{M}$  interfering compounds presence in food samples in an electrochemical cell containing 0.1 M PBS (pH 7.0), at applied potentials from 0.40 V to 1.15 V in scan rate of 25  $\text{mVs}^{-1}$ .

Substance	Added ( $\mu\text{M}$ )	Electrocatalytic peak current ( $\mu\text{A}$ )	RSD
GPh	10	1.2724	$\pm 0.0074$
Parathion	40	0.0339	$\pm 0.0017$
Chlorpyrifos	40	0.0527	$\pm 0.0019$
Dipterex	40	0.0246	$\pm 0.0015$
Ethion	40	0.0462	$\pm 0.0022$
Deltamethrin	40	0.0903	$\pm 0.0017$
Dichlorvos	40	0.0742	$\pm 0.0015$
Acetochlor	40	0.0651	$\pm 0.0019$
$\text{Mg}^{2+}$	40	0.0255	$\pm 0.0012$
$\text{Ag}^+$	40	0.0392	$\pm 0.0012$
$\text{Fe}^{2+}$	40	0.0125	$\pm 0.0015$
$\text{Na}^+$	40	0.0275	$\pm 0.0011$
$\text{Ca}^{2+}$	40	0.0125	$\pm 0.0013$
$\text{Al}^{3+}$	40	0.0222	$\pm 0.0012$
$\text{CO}_4^{2-}$	40	0.0401	$\pm 0.0014$
$\text{NH}_4^+$	40	0.0509	$\pm 0.0015$
$\text{CO}_3^{2-}$	40	0.0178	$\pm 0.0017$
$\text{NO}_3^-$	40	0.0122	$\pm 0.0016$

To assess the applicability and validity of the MIP@GO/GCE as GPh sensor in food samples, the DPV response of MIP@GO/GCE under consecutive injections of 0.1  $\mu\text{M}$  GPh solutions in an electrochemical cell containing 0.1M PBS prepared from corn samples, at applied potentials from 0.40 V to 1.15 V in  $25\text{mVs}^{-1}$  scan rate were investigated. Glyphosate ELISA Plate Kit was used for determination GPh in prepared real specimens before and after adding GPh. The attained analytical via standard addition technique are summarized in Table 3 which shows the great conformity between the results of both analyses, and the obtained recovery (97.00% to 98.25%) and RSD (3.58% to 4.25%) values are acceptable. It reflects the appropriate accuracy and validity of results of MIP@GO/GCE for the determination of GPh level in food samples.

**Table 3.** Analytical results from the determination of GPh into prepared real specimens of corn samples

Spiked( $\mu\text{M}$ )	DPV			Glyphosate ELISA Plate Kit		
	Detected( $\mu\text{M}$ )	Recovery(%)	RSD(%)	Detected( $\mu\text{M}$ )	Recovery(%)	RSD(%)
0.00	0.00	--	4.25	0.00	--	4.21
0.100	0.097	97.00	4.17	0.096	96.00	4.18
0.200	0.194	97.00	3.58	0.197	98.50	3.76
0.300	0.295	98.25	3.85	0.294	98.00	4.04

#### 4. CONCLUSION

The aim of this work was the preparation of MIP@GO/GCE as an electrochemical sensor for monitoring GPh content in corn. The nanocomposite were prepared through the polymerization of pyrrole on GO nanosheets. The structural studies indicated to effective polymerization PPy on the surface of GO. Electrochemical analyses demonstrated that MIP@GO/GCE showed the sensitive and selective electrocatalytic response to GPh in electrochemical cell, and indicated the sensitivity of  $0.1271 \mu\text{A}/\mu\text{M}$  and a stable linear range from 0 to  $1800 \mu\text{M}$ . The sensor for GPh reached a low detection limit of  $11 \mu\text{M}$ . The results revealed that MIP@GO/GCE possessed a broad linear range and relatively low detection limit value between the recent GPh sensors. It can be related to a synergism exists between the GO and MIP, that can provide electro-conducting path and excellent surface-to-volume to promote the accessibility of the GPh molecule to the binding sites and cavities and facilitate the electron transfer rate. The applicability and validity of the MIP@GO/GCE as GPh sensor in food samples were examined and results exhibited that the obtained recovery and RSD values were acceptable. It reflected the appropriate accuracy and validity of results of MIP@GO/GCE for the determination of GPh level in food samples.

#### ACKNOWLEDGEMENT

This research was supported in part by Scientific and technology development programme of Jilin Province, China (20210202005NC).



## References

1. W.S. Xiang, X.J. Wang, T.R. Ren and X.L. Ju, *Pest Management Science: formerly Pesticide Science*, 61 (2005) 402.
2. L. Nan, C. Yalan, L. Jixiang, O. Dujuan, D. Wenhui, J. Rouhi and M. Mustapha, *RSC Advances*, 10 (2020) 27923.
3. A. Samsel and S. Seneff, *Entropy*, 15 (2013) 1416.
4. H. Karimi-Maleh, H. Beitollahi, P.S. Kumar, S. Tajik, P.M. Jahani, F. Karimi, C. Karaman, Y. Vasseghian, M. Baghayeri and J. Rouhi, *Food and Chemical Toxicology*, (2022) 112961.
5. R. Mesnage, N. Defarge, J.S. De Vendômois and G. Séralini, *Food and Chemical Toxicology*, 84 (2015) 133.
6. W. Zheng, X. Liu, X. Ni, L. Yin and B. Yang, *IEEE access*, 9 (2021) 91476.
7. M. Yang, C. Li, Y. Zhang, D. Jia, X. Zhang, Y. Hou, R. Li and J. Wang, *International Journal of Machine Tools and Manufacture*, 122 (2017) 55.
8. J.P.K. Gill, N. Sethi, A. Mohan, S. Datta and M. Girdhar, *Environmental Chemistry Letters*, 16 (2018) 401.
9. S. Changaei, J. Zamir-Anvari, N.-S. Heydari, S.G. Zamharir, M. Arshadi, B. Bahrami, J. Rouhi and R. Karimzadeh, *Journal of Electronic Materials*, 48 (2019) 6216.
10. W. Zheng, L. Yin, X. Chen, Z. Ma, S. Liu and B. Yang, *Pattern Recognition*, 120 (2021) 108153.
11. R. Li, X. Qian, C. Gong, J. Zhang, Y. Liu, B. Xu, M.S. Humayun and Q. Zhou, *IEEE Transactions on Biomedical Engineering*, (2022) 1.
12. S. Carlisle and J. Trevors, *Water, Air, and Soil Pollution*, 39 (1988) 409.
13. X. Zhang, C. Li, Y. Zhang, D. Jia, B. Li, Y. Wang, M. Yang, Y. Hou and X. Zhang, *The International Journal of Advanced Manufacturing Technology*, 86 (2016) 3427.
14. Y. Zhu, F. Zhang, C. Tong and W. Liu, *Journal of chromatography A*, 850 (1999) 297.
15. B.S. Clegg, G.R. Stephenson and J.C. Hall, *Journal of Agricultural and Food Chemistry*, 47 (1999) 5031.
16. Z.-X. Guo, Q. Cai and Z. Yang, *Journal of Chromatography A*, 1100 (2005) 160.
17. F. Sun, L. Yang, S. Li, Y. Wang, L. Wang, P. Li, F. Ye and Y. Fu, *Journal of Agricultural and Food Chemistry*, 69 (2021) 12661.
18. S. Wang, B. Liu, D. Yuan and J. Ma, *Talanta*, 161 (2016) 700.
19. P.L. Alferness and Y. Iwata, *Journal of Agricultural and Food Chemistry*, 42 (1994) 2751.
20. E. Çetin, S. Şahan, A. Ülgen and U. Şahin, *Food chemistry*, 230 (2017) 567.
21. C.T. Thanh, P.N.D. Duoc, N.T. Huyen, V.T. Thu, N.X. Nghia, N.H. Binh, P. Van Trinh, N. Van Tu, C.T. Anh, V.C. Tu, P.N. Minh, H. Abe, E.D. Obraztsova and N. Van Chuc, *Diamond and Related Materials*, 128 (2022) 109312.
22. M.-B. Gholivand, A. Akbari and L. Norouzi, *Sensors and Actuators B: Chemical*, 272 (2018) 415.
23. C. Zhang, X. Liang, Y. Lu, H. Li and X. Xu, *Sensors*, 20 (2020) 4146.
24. S. Pintado, R.R. Amaro, M. Mayén and J.M.R. Mellado, *International Journal of Electrochemical Science*, 7 (2012) 305.
25. P.F.P. Barbosa, E.G. Vieira, L.R. Cumba, L.L. Paim, A.P.R. Nakamura, R.D.A. Andrade and D. Ribeiro, *International Journal of Electrochemical Science*, 14 (2019) 3418.
26. H. Karimi-Maleh, C. Karaman, O. Karaman, F. Karimi, Y. Vasseghian, L. Fu, M. Baghayeri, J. Rouhi, P. Senthil Kumar and P.-L. Show, *Journal of Nanostructure in Chemistry*, 12 (2022) 429.
27. C. Sheng, G. He, Z. Hu, C. Chou, J. Shi, J. Li, Q. Meng, X. Ning, L. Wang and F. Ning, *Journal of Engineered Fibers and Fabrics*, 16 (2021) 1925832385.
28. M. Qu, Z. Chen, Z. Sun, D. Zhou, W. Xu, H. Tang, H. Gu, T. Liang, P. Hu and G. Li, *Nano Research*, (2022) 1.
29. M. Yu, L. Wu, J. Miao, W. Wei, A. Liu and S. Liu, *Analytica Chimica Acta*, 1080 (2019) 84.

30. T. Sajini, M. Gigimol and B. Mathew, *Journal of Polymer Research*, 26 (2019) 1.
31. K. Wang, S. Gao, C. Lai, Y. Xie, Y. Sun, J. Wang, C. Wang, Q. Yong, F. Chu and D. Zhang, *Industrial Crops and Products*, 187 (2022) 115366.
32. Q.T. Ain, S.H. Haq, A. Alshammari, M.A. Al-Mutlaq and M.N. Anjum, *Beilstein Journal of Nanotechnology*, 10 (2019) 901.
33. W. Zhang, X. Guan, X. Qiu, T. Gao, W. Yu, M. Zhang, L. Song, D. Liu, J. Dong and Z. Jiang, *Applied Surface Science*, 610 (2023) 155290.
34. W. Dang, J. Guo, M. Liu, S. Liu, B. Yang, L. Yin and W. Zheng, *Applied Sciences*, 12 (2022) 9213.
35. S.C. Canobre, F.F. Xavier, W.S. Fagundes, A.C.D. Freitas and F.A. Amaral, *Journal of Nanomaterials*, 2015 (2015) 1.
36. H. Karimi-Maleh, R. Darabi, M. Shabani-Nooshabadi, M. Baghayeri, F. Karimi, J. Rouhi, M. Alizadeh, O. Karaman, Y. Vasseghian and C. Karaman, *Food and Chemical Toxicology*, 162 (2022) 112907.
37. M. Yang, C. Li, Y. Zhang, D. Jia, R. Li, Y. Hou, H. Cao and J. Wang, *Ceramics International*, 45 (2019) 14908.
38. M. Liu, C. Li, Y. Zhang, M. Yang, T. Gao, X. Cui, X. Wang, W. Xu, Z. Zhou and B. Liu, *Chinese Journal of Aeronautics*, (2022) 1.
39. S.-J. Sun, P. Deng, C.-E. Peng, H.-Y. Ji, L.-F. Mao and L.-Z. Peng, *Polymers*, 14 (2022) 2899.
40. J. Zhang, C. Li, Y. Zhang, M. Yang, D. Jia, G. Liu, Y. Hou, R. Li, N. Zhang and Q. Wu, *Journal of Cleaner Production*, 193 (2018) 236.
41. Y. Zhang, C. Li, M. Yang, D. Jia, Y. Wang, B. Li, Y. Hou, N. Zhang and Q. Wu, *Journal of Cleaner Production*, 139 (2016) 685.
42. J.S. Santos, M.S. Pontes, E.F. Santiago, A.R. Fiorucci and G.J. Arruda, *Science of the Total Environment*, 749 (2020) 142385.
43. Z. Wang, L. Dai, J. Yao, T. Guo, D. Hrynsphan, S. Tatsiana and J. Chen, *Bioresource Technology*, 327 (2021) 124785.
44. T. Gao, Y. Zhang, C. Li, Y. Wang, Y. Chen, Q. An, S. Zhang, H.N. Li, H. Cao and H.M. Ali, *Frontiers of Mechanical Engineering*, 17 (2022) 1.
45. R. Dalvand, S. Mahmud and J. Rouhi, *Materials Letters*, 160 (2015) 444.
46. Y. Xie, S. Gao, Z. Ling, C. Lai, Y. Huang, J. Wang, C. Wang, F. Chu, F. Xu and M.-J. Dumont, *Journal of Materials Chemistry A*, (2022) 1.
47. B. Fan, X. Zhao, Z. Liu, Y. Xiang and X. Zheng, *Sustainable Chemistry and Pharmacy*, 29 (2022) 100821.
48. R. Li, Z. Du, X. Qian, Y. Li, J.-C. Martinez-Camarillo, L. Jiang, M.S. Humayun, Z. Chen and Q. Zhou, *Quantitative Imaging in Medicine and Surgery*, 11 (2021) 918.
49. G. Yasin, M. Arif, T. Mehtab, M. Shakeel, M.A. Mushtaq, A. Kumar, T.A. Nguyen, Y. Slimani, M.T. Nazir and H. Song, *Inorganic Chemistry Frontiers*, 7 (2020) 402.
50. C. Liu and J. Rouhi, *RSC Advances*, 11 (2021) 9933.
51. W. Zheng, X. Liu and L. Yin, *Applied Sciences*, 11 (2021) 1316.
52. X. Wu, *Microchimica Acta*, 176 (2012) 23.
53. J. Rouhi, M.R. Mahmood, S. Mahmud and R. Dalvand, *Journal of Solid State Electrochemistry*, 18 (2014) 1695.
54. M. Shi, H. Zhu, C. Chen, J. Jiang, L. Zhao and C. Yan, *International Journal of Minerals, Metallurgy and Materials*, 30 (2023) 25.
55. J.L. da Silva, E. Buffon, M.A. Beluomini, L.A. Pradela-Filho, D.A.G. Araújo, A.L. Santos, R.M. Takeuchi and N.R. Stradiotto, *Analytica Chimica Acta*, 1143 (2021) 53.
56. H. Setiyanto, S. Rahmadhani, S. Sukandar, V. Saraswati, M.A. Zulfikar and N. Mufti, *Int. J. Electrochem. Sci*, 15 (2020) 5477.
57. X. Cui, C. Li, Y. Zhang, Z. Said, S. Debnath, S. Sharma, H.M. Ali, M. Yang, T. Gao and R. Li,

- Journal of Manufacturing Processes*, 80 (2022) 273.
58. S. Lu, J. Guo, S. Liu, B. Yang, M. Liu, L. Yin and W. Zheng, *Applied Sciences*, 12 (2022) 9529.
  59. X. Wang, C. Li, Y. Zhang, H.M. Ali, S. Sharma, R. Li, M. Yang, Z. Said and X. Liu, *Tribology International*, 174 (2022) 107766.
  60. W. Chen, Z. Guo, Q. Ding, C. Zhao, H. Yu, X. Zhu, M. Fu and Q. Liu, *Polymer*, 215 (2021) 123384.
  61. J. Rouhi, H.K. Malayeri, S. Kakooei, R. Karimzadeh, S. Alrokayan, H. Khan and M.R. Mahmood, *International Journal of Electrochemical Science*, 13 (2018) 9742.
  62. M. Shi, R. Wang, L. Li, N. Chen, P. Xiao, C. Yan and X. Yan, *Advanced Functional Materials*, (2022) 2209777.
  63. C. Dong, H. Shi, Y. Han, Y. Yang, R. Wang and J. Men, *European Polymer Journal*, 145 (2021) 110231.
  64. S. Hou, B. Shen, D. Zhang, R. Li, X. Xu, K. Wang, C. Lai and Q. Yong, *Bioresource Technology*, 362 (2022) 127825.
  65. W. Xu, C. LI, Y. Zhang, H.M. Ali, S. Sharma, R. Li, M. Yang, T. Gao, M. Liu and X. Wang, *International Journal of Extreme Manufacturing*, 4 (2022) 042003.
  66. M. Regiart, A. Kumar, J.M. Gonçalves, G.J. Silva Junior, J.C. Masini, L. Angnes and M. Bertotti, *ChemElectroChem*, 7 (2020) 1558.
  67. C.T. Thanh, N.H. Binh, P.N.D. Duoc, V.T. Thu, P. Van Trinh, N.N. Anh, N. Van Tu, N.V. Tuyen, N. Van Quynh, V.C. Tu, B.T.P. Thao, P.D. Thang, H. Abe and N. Van Chuc, *Bulletin of Environmental Contamination and Toxicology*, 106 (2021) 1017.
  68. S. Wang, Y. Yao, J. Zhao, X. Han, C. Chai and P. Dai, *RSC advances*, 12 (2022) 5164.
  69. C.-m. Dai, S.-U. Geissen, Y.-l. Zhang, Y.-j. Zhang and X.-f. Zhou, *Journal of hazardous materials*, 184 (2010) 156.
  70. F. Husairi, J. Rouhi, K. Eswar, A. Zainurul, M. Rusop and S. Abdullah, *Applied Physics A*, 116 (2014) 2119.